Int. J. Advanced Design and Manufacturing Technology, 2025, Vol. 18, No. 4, pp. 1-9

DOI: *ISSN: 2252-0406* *https://admt.isfahan.iau.ir*

Three-Dimensional Finite Element Analysis of Equivalent Plastic Strain Distribution and Compressive Residual Stress in the Surface Mechanical Attrition Treatment Process of AZ31 Magnesium Alloy

Ali Kazemi, Ali Heidari *, Kamran Amini, Farshid Aghadavoudi, Mohsen Loh-Mousavi

Department of Mechanical Engineering, Kho. C., Islamic Azad University, Khomeinishahr, Iran

E-mail: en_alikazemi975@yahoo.com, ali_heidari@iau.ac.ir, kamini@iau.ac.ir, davoodi@iaukhsh.ac.ir, loh-mousavi@iaukhsh.ac.ir

*Corresponding Author

Received: 15 July 2025, Revised: 28 August 2025, Accepted: 8 September 2025

Abstract: Surface Mechanical Attrition Treatment (SMAT) is a process in which the surface of a component is enhanced by the impact of small steel shots, creating a thin nanostructured layer that improves the mechanical properties of metallic materials. In this process, significant plastic deformation initially occurs due to the impact of steel shots on the surface, and after each shot rebounds, compressive residual stress is generated on the surface. This study numerically investigates the effect of shot size and speed of shot balls on equivalent plastic strain profiles, residual stress depth, and maximum compressive residual stress during the SMAT process of AZ31material using the Finite Element Method (FEM). The plastic deformation process during SMAT was analyzed using ABAQUS Explicit Software. The Explicit Dynamic solver was employed to analyze the effects of shot velocity and diameter using FEM. The results indicated that the maximum compressive residual stress increased from 202 MPa to 205 MPa as the shot diameter increased from 1 mm to 3 mm at a velocity of 10 m/s, while an increase in velocity from 4 m/s to 10 m/s at a shot diameter of 1 mm resulted in an increase in maximum compressive residual stress from 155 MPa to 202 MPa. The results suggest that shot velocity has a significant effect on residual stress, whereas shot diameter has less impact. The change in plastic strain due to shot diameter is less influential than shot velocity. With the help of the method developed in this study, it is possible to achieve the effects of effective parameters in the process, which are very difficult and expensive to achieve with practical methods.

Keywords: AZ31 Magnesium Alloy, Finite Element Method, Residual Stress, SMAT

Biographical notes: Ali Kazemi received his PhD in Mechanical Engineering in 2024. **Ali Heidari** is an Associate Professor at the Department of Mechanical Engineering, Khomeinishahr Branch, Islamic Azad University, Isfahan, Iran. **Kamran Amini** is an Associate Professor at the Department of Mechanical Engineering, Khomeinishahr Branch, Islamic Azad University, Isfahan, Iran. **Farshid Aghadavoudi** is an Associate Professor at the Department of Mechanical Engineering, Khomeinishahr Branch, Islamic Azad University, Isfahan, Iran. **Mohsen Loh-Mousavi** is an Assistant Professor at the Department of Mechanical Engineering, Khomeinishahr Branch, Islamic Azad University, Isfahan, Iran.

Research paper

1 INTRODUCTION

SMAT is an effective technique that enhances the mechanical properties of metal by inducing surface nano crystallization. During this process, spherical shots with high kinetic energy are randomly and continuously impacted onto the surface of a sample multiple times within a chamber by an ultrasonic generator [1-2]. Each shot creates a plastic zone with permanent deformation, surrounded by an elastic region that has not yet reached the plastic limit and remains elastically deformed. This elastic region tends to return to its original state, exerting pressure on the plastic zone, thereby generating compressive residual stress. The multiplicity and overlap of these indentations eventually result in the formation of a layer with compressive residual stress on the surface of the component. This layer significantly enhances the fatigue strength of the component. Therefore, predicting the shape and magnitude of the subsurface residual stress distribution after the SMAT process is of great importance [3-4]. Shot velocity can vary depending on the applied vibration frequency, amplitude, chamber geometry, and shot properties. Shot velocity is the most critical parameter in surface treatment using the SMAT process, and the height and diameter of the SMAT device chamber directly affect shot velocity. Therefore, many researchers have considered shot velocity as the average speed in the SMAT process. In a study, Zhang et al. [5] examined the effect of the SMAT process on the surface of AISI 304 steel using a numerical simulation based on the Johnson-Cook method. Based on the simulation results, the distribution of residual stress was investigated, and the impact of impact frequency and shot size on compressive residual stress was analyzed. The findings indicated that when the only variable parameter is the SMAT process intensity, it effectively means a change in velocity. The depth of residual stress penetration increases significantly with intensity, and the maximum compressive residual stress also slightly increases. Meguid et al. [6] conducted a comprehensive nonlinear dynamic analysis involving an elastoplastic target material and the impact of two shots with varying central distances from each other. The results demonstrated that decreasing the central distance between the two shots increases the depth of the compacted layer due to the overlapping effects of the shots on the surface. They compared double and single impacts on the target material's surface, showing that first, the dynamic friction coefficient has no effect on residual stress distribution, and second, multiple impacts have a significant influence on achieving uniform residual stress distribution across the surface and depth of the target material. For the vibration chamber, Todaka et al. [7] selected an amplitude of 90 micrometers, a frequency of 20 kHz, and a throw distance of 10 mm, claiming that shot velocity could be less than 20 m/s. Chaise et al. [8] used a piezoelectric transducer with a frequency of 20 kHz, setting the amplitude of vibration at 25 micrometers, the vibration chamber height at 50 mm, and the average shot velocity for the numerical model at 4 m/s. Astaraee et al. [9] set the average shot velocity in the vibration chamber at 3.6 m/s in a numerical model. Yin et al. [10] considered the average shot velocity in their study to be 3.6 m/s. Manchoul et al. [11] determined the average shot velocity to be 4 and 8 m/s for two different amplitudes of 32 and 64 micrometers and a constant frequency of 20 kHz. Meng et al. [12] investigated the deformation behavior of AZ31 magnesium alloy using the SMAT process, revealing that the surface grain size reached the nanoscale, with grain size decreasing near the surface and becoming less apparent in the layers closer to the core until it disappeared. Zhang et al. [13] studied the effect of surface mechanical attrition on the nanostructured layers of AISI 304 stainless steel. According to their experiments, the nanostructure was successfully fabricated on the surface layers. XRD results showed that the peak heights were shorter and broader, indicating grain refinement, which led to improved mechanical properties. In another study, Bagherifard et al. [14] investigated the impact of shot peening on the structural behavior of titanium by combining finite element simulations with experimental tests. They calculated factors such as residual stress and X-ray diffraction patterns, concluding that the formation of small crystal regions on the shot impact surfaces leads to improved material strength. Anand Kumar et al. studied the effects of SMAT treatment on the fatigue life of alloy 718. SMAT was performed in vacuum with 5 mm diameter steel balls for 30 and 60 min at a vibration frequency of 50 Hz. SMAT resulted in increased tensile strength, decreased ductility, and increased fatigue life. According to their results, no significant difference was observed between the fatigue life of samples with SMAT times of 30 and 60 seconds.[15]. Given the high cost of experimental tests and the complexity of the SMAT process, numerical simulation methods have been used to examine the influential parameters in this process. For example, investigating the effect of each frequency would require designing a new tool, which involves design challenges and additional costs. Therefore, researchers have tended towards numerical studies [16-21]. Consequently, a highly practical approach to solving such issues is the use of finite element methods. The aim of this study is to statistically analyze the effects of shot diameter and velocity in the SMAT process on residual stress variations and to examine the plastic strain profiles of AZ31 magnesium alloy. In this research, numerical simulations were conducted using an explicit dynamics solver, and residual stress on the surface and in-depth was assessed using the results of finite element simulations.

2 MATERIALS AND METHODS

Considering the nature of the process, which affects the metal surface, shot peening (SP) and SMAT are practically similar; however, the SMAT process differs from the shot peening process in terms of its principles and methods. In the SMAT process, several ball shots impact on surface of the target material. The shot velocities in the SMAT process (generally ranging from 1 to 20 m/s) are lower compared to those in shot peening (usually 20 to 150 m/s). This difference in velocity can lead to a reduction in the energy delivered by the impacting shot, especially in the case of smaller shots. However, to compensate for the lower energy resulting from the reduced velocity in the SMAT process, larger shots are used. During SMAT, ultrasonic vibration at a high frequency of over 20 kHz causes the shots to continuously and randomly impact the sample surface [22-23]. Given the very high strains and strain rates at relatively low temperatures, the SMAT process exposes the surface of the material to severe plastic deformation, leading to the formation of ultrafine-grained or nanostructured surfaces [24-25].

The numerical model of the SMAT process is quite complex, as it involves the dynamic analysis of rapidly moving impacting balls on a metal target, which itself may have a complex geometry. Since SMAT involves random, high-velocity impacts of spherical shots, FEA helps to predict the mechanical effects, such as plastic deformation, residual stress distribution, grain refinement zones, and hardness gradients.

In this study, the target material is AZ31 magnesium alloy. Magnesium, due to its low density and favorable chemical and mechanical properties, has various alloy compositions with numerous industrial applications. AZ31 is a magnesium alloy containing 3 weight percent aluminum (Al) and 1 weight percent zinc (Zn) [26-27]. "Table 1" shows the composition of AZ31 material as a magnesium alloy.

Table 1 The weight percentages (wt%) of the AZ31.

Element	Mg	Ni	Mn	Zn	Al
Composition	Bal.	0.03	0.25	0.71	3.1

To achieve the research objectives, the finite element software ABAQUS is used for simulations. In this study, as shown in "Fig.1", three components are modeled in ABAQUS as: 1) a circular plate with a diameter of 21 mm and a thickness of 3 mm, 2) a vibration chamber modeled as a closed and hollow cylinder with a diameter of 22 mm, and 3) balls with three different diameters (all dimensions are based on real samples). A total of 12 balls are placed on the vibrating platform to cover the underside of the vibration chamber.

In real conditions, stainless steel balls are used for the SMAT process, and the mechanical properties of AZ31 plate are much weaker than steel. Therefore, in finite element simulation, to reduce simulation time, both the vibration chamber and the balls are defined as rigid materials. In contrast, the plate is defined as deformable, as the focus is on analyzing the plate.

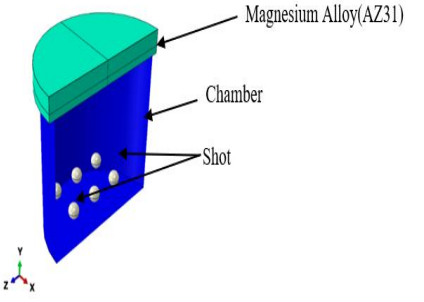

Fig. 1 Simulation display of the assembly: vibrating platform, target material (AZ31), and balls.

"Table 2" shows the parameter values used in the finite element simulation of the structure, including the geometric and mechanical properties of the AZ31 plate and stainless-steel balls. These parameters were defined in the ABAQUS software toolboxes. The mechanical properties of the AZ31 are reported in "Table 3". To determine the yield stress of the material, an experimental tensile test was conducted, and the engineering stress-strain results were extracted in Excel format. The plastic behavior of the material was defined using the true stress-strain curve. Additionally, the material was modeled as homogeneous and isotropic.

Table 2 The parameter values and geometric and mechanical properties of the 3D FEA simulated model

Parameter	Value
Simulation Time	10 milliseconds
Sheet Size (Target material)	Diameter: 21(mm), Thickness: 3(mm)
Ball Speeds	4 m/s, 8 m/s, 10 m/s
Ball Diameters	1mm, 2mm, 3mm
Ball Property	Density: 7800 (kg/m^3)
Target Material (AZ31) Properties	Density: 1770 (kg/m^3) Young's Modulus: 45 (GPa) Poisson's Ratio: 0.3

Table 3 Mechanical properties of AZ31 magnesium alloy used in modeling

Parameter	Value
Young's Modulus	45 (GPa)
Yield Strength	285 (MPa)
Tensile Strength	313 (MPa)
Elongation (%)	18%

Given the transfer of kinetic energy through the vibrating platform at the bottom of the SMAT chamber, it can be inferred that the shots move along a directed path with an impact angle very close to 90 degrees, and negligible interactions between the shots can be ignored. The shot impact velocity was estimated by finite element modeling of 1, 2, and 3 mm shots within a cylindrical chamber representing the device's chamber. The actual dimensions of the chamber were considered in the modeling. As shown in "Fig. 2", in the SMAT device, the vibrational signal generated by the ultrasonic generator is in the form of a harmonic sine function, which was modeled as a boundary condition using Equation (1):

$$x(t) = A \sin \omega t \quad (1)$$

Impact Conditions are performed as follows:

- Impact angle: Often normal (90°) for simplicity, but can vary.
- Single or multiple sequential impacts simulated.
- Dynamic, explicit time integration is usually necessary (due to high-speed impact).

ABAQUS/Explicit was used for the 3D Finite Element Simulation of the process. Several outputs, such as Residual stress distribution (depth & magnitude), Plastic strain distribution, and Equivalent von Mises stress, were obtained. Fine mesh was used near the impact area for accuracy, and a Coarser mesh away from the impact zone to reduce computational cost. The Path-FE method was used to extract the residual stresses along a predefined path (vertical from the impact point into the depth of the substrate). This path was selected through the center of the impact zone in the 3D model. After the simulation completes, the residual stress is extracted node-by-node along this path. The principal stresses, also known as von Mises stresses, were plotted against depth. No additional sub-modeling or cell division was needed.

The contact between the sheet surface and the balls was defined using a penalty contact method (frictional contact). The coefficient of friction between the sheet and the balls was set to μ=0.1, with hard contact behavior used in the vertical direction. To investigate the effect of the element size, a sensitivity analysis was performed. The simulation process was carried out using a mesh of elements with a size of 0.25 mm to determine the maximum residual stress induced in the sheet. According to experimental testing in the SMAT process, the chamber floor oscillates based on Equation (1). Ultrasonic vibration was defined as a harmonic sine function for the vibration chamber. In the simulation, vibration was initially applied to the platform so that the balls would impact the sheet and induce stress on it. In the subsequent stage, vibration and loading were removed to allow for the measurement of residual stresses in the free body.

To study the effects of speed and ball size on the SMAT process, two test scenarios were considered. The investigation includes three different speeds (4, 8, and 10 m/s) and three ball sizes (1, 2, and 3 millimeters in diameter) according to SAE J444 standards. The analysis and boundary conditions are entered into specific parts of the ABAQUS software. After inputting all the parameters into the software, the analysis and evaluation of the results are performed.

3 RESULTS AND DISCUSSION

In this study, the effects of diameter and speed on residual compressive stress, depth of residual compressive stress, and maximum equivalent plastic strain were investigated in SMAT process. The analysis was performed through finite element simulations, and the results are presented in "Table 4".

Table 4 Characteristics of the samples and main results of finite element models

Case Study No.	Ball Diameter (mm)	speed (m/s)	Maximum compressive Residual Stress (MPa)	Maximum Equivalent Plastic Strain
1	1	4	-155	0.064
2	1	8	-166	0.073
3	1	10	-202	0.079
4	2	4	-173	0.065
5	2	8	-182	0.073
6	2	10	-203	0.080
7	3	4	-176	0.066
8	3	8	-190	0.073
9	3	10	-205	0.080

As shown in "Table 4", residual stresses in two conditions and nine models were examined. After performing the simulation and analysis with ABAQUS, the outputs, including stress histories (Smises, Smax, Smin) and equivalent plastic strain (PEEQ) in different directions, as well as the thickness of the sheet sample for all time steps during the defined process duration, were obtained. Figure 2 displays the deformed sample, the graphical distribution of stress, equivalent plastic strain, and displacement.

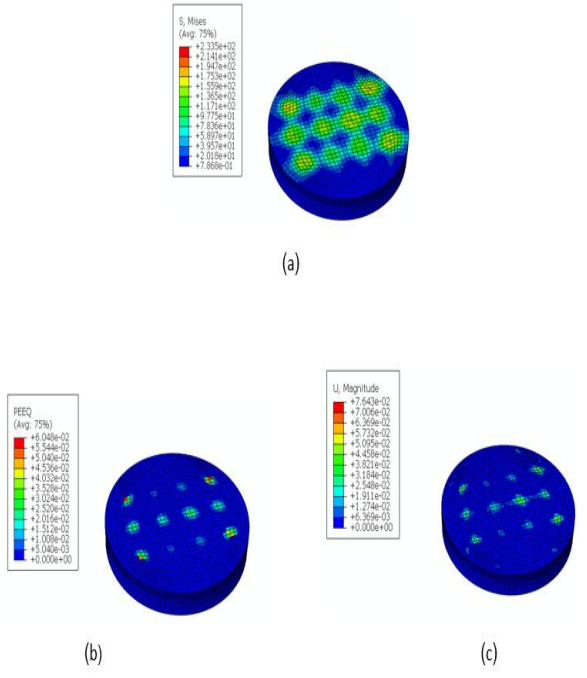

Fig. 2 Results from the simulation, a) distribution of von Mises stress, b) distribution of equivalent plastic strain, c) displacement.

The process involves numerous parameters that need to be controlled to achieve a suitable residual stress distribution on the workpiece. Therefore, the effect of ball diameter and speed on residual stress distribution (Section 4-1) and the effect of ball diameter and speed on equivalent plastic strain (Section 4-2) will be examined.

3.1. Influence of Ball Diameter and Speed on Compressive Residual Stress

3.1.1. Effect of Ball Diameter on Residual Stress

To investigate the effect of ball diameter on the residual stress curve, three different diameters, 1mm, 2 mm, and 3 mm, are considered. The impact speed is set at 4 m/s. Figure 3 shows the residual stress distribution along the depth of the compacted layer in the direction of the impact. It can be observed that the maximum absolute residual stress is 155 MPa, 173 MPa, and 176 MPa, respectively, for the different ball diameters 1, 2 and 3mm. The differences between the results for the various ball diameters are relatively close.

As the ball diameter increases, the maximum compressive residual stress gradually increases, while the depth affected by the residual stress shows a significant increase. The results of this study are in good agreement with the research conducted by Meguid and colleagues [6]. In another study, Meguid et al. [28] examined the influence of speed, size, shape, and number of balls in the shot-peening process on a metal workpiece. The results showed that with an increase in ball speed, the stress applied to the subsurface increases, and the stress penetrates deeper layers. This study demonstrates that each particle's impact on the workpiece increases the applied surface stress in the simulation. Additionally, the size of the particles has a direct relationship with the intensity of the stress applied to the surface of the workpiece and with the depth of stress penetration, such that as the ball diameter increases, the depth of stress penetration also increases.

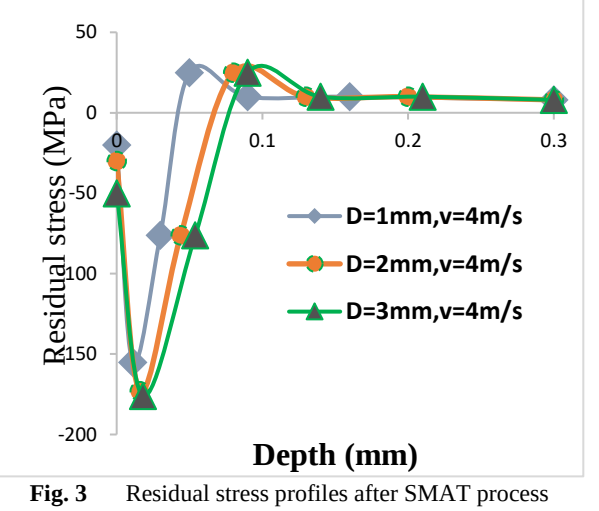

Fig. 3 Residual stress profiles after SMAT process (diameters: 1, 2, and 3 mm at 4 m/s speed).

3.1.2. Effect of Ball Speed on Residual Stress of The Target Material

Figure 4 illustrates the residual stress distribution along the depth of the compacted layer in the direction of impact for different diameters and speeds. As the speed increases, the depth of the compressive residual stress zone slightly increases. The impact speed significantly affects the surface stress and the maximum subsurface stress. It is observed that increasing the speed from 4 m/s to 10 m/s for a 1 mm diameter ball increases the compressive residual stress from 155 MPa to 205MPa. This increase could be related to greater work hardening resulting from the higher impact force at greater speeds. The results indicate that increasing ball speed has a more significant impact on compressive residual stress compared to increasing ball diameter. As one moves towards the depth of the sample, it is evident that with the increase in impact speed, the depth of the plastic zone and compressive stress on the surface, along with the maximum residual stress at depth, will increase.

The increase in the maximum compressive residual stress and the depth of the compacted layer due to higher ball speed is more noticeable than that due to ball diameter.

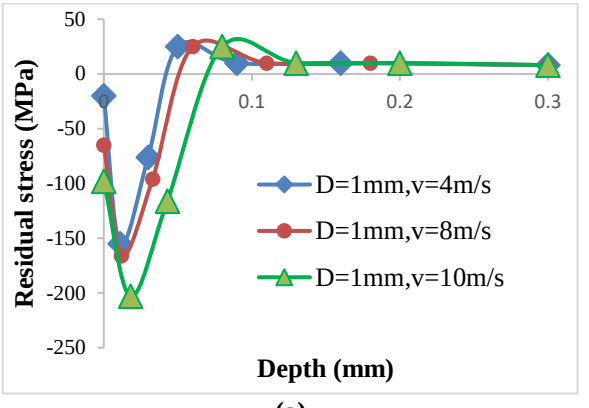

(a)

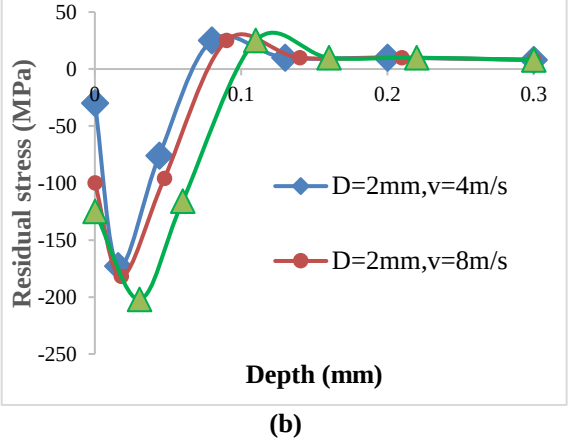

(b)

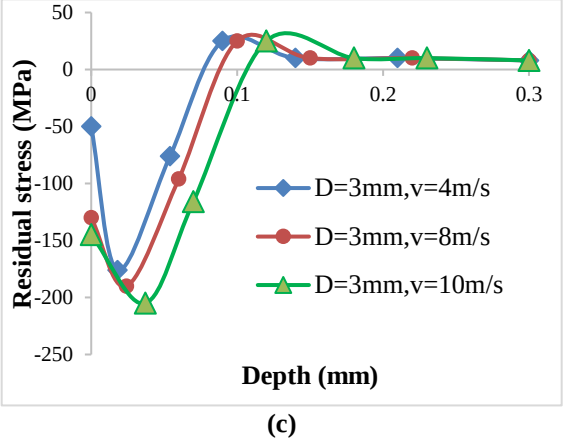

(c)

Fig. 4 Residual stress profiles after SMAT Process at various speeds for ball diameters: (a): 1mm, (b): 2mm, and (c): 3mm.

The trend of results of this study are in agreement with the research conducted by Majzoobi et al. [16]. They used LS-DYNA finite element simulation to examine the impact of several balls (9, 13, and 25 in number) arranged in different configurations at various speeds ranging from 50 to 100 m/s. They observed that the maximum compressive residual stress occurred when 25 balls impacted at a speed of 90 m/s, reaching a value of up to 1100 MPa. They demonstrated that ball speed significantly influences the maximum compressive residual stress.

3.2. Influence of Ball Diameter and Speed on Equivalent Plastic Strain

4.2.1. Effect of Ball Diameter on Equivalent Plastic Strain

Equivalent plastic strain is a key parameter for surface densification and grain boundary production [29-30]. Figure 5 shows the plastic strain profile in the depth of the compressed layer along the impact direction for different ball diameters (1, 2, and 3 mm) at a speed of 4 m/s. The ball size significantly affects the depth of the affected area where plastic deformation occurs, but it has a minimal impact on the maximum equivalent plastic strain. As the ball diameter increases from 1 mm to 3 mm, the maximum plastic strain changes from 0.06 to about 0.07. This result aligns well with the study by Yarar et al.[18], who investigated the multiple ball impacts due to the SMAT process in aluminum alloy 7075 to achieve maximum equivalent stress, equivalent plastic strain, residual stress depth, and maximum compressive residual stress. It was observed that ball size is not as influential as ball speed on maximum equivalent stress. The findings indicate that increasing ball diameter and speed leads to an increase in residual stress, showing a similar and incremental trend, consistent with the results of this study and the dynamic finite element analysis on single-impact plastic deformation behavior in aluminum alloy 7075 as presented in reference [18].

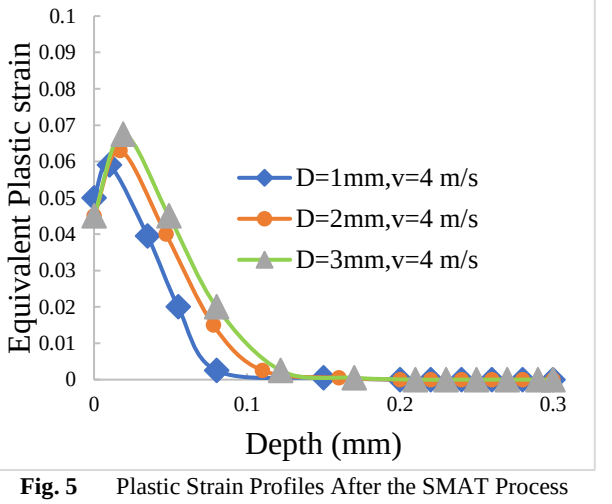

Fig. 5 Plastic Strain Profiles After the SMAT Process (Diameters of 1, 2, and 3 mm at a Speed of 4 m/s).

3.2.2. Effect of Ball Speed on Effective Plastic Strain

Figure 6 shows the equivalent plastic strain profiles for a 1 mm diameter shot at speeds of 4, 8, and 10 m/s along the depth.

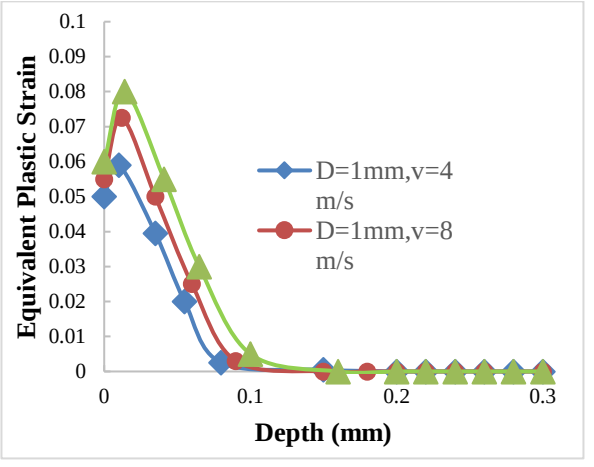

Fig. 6 Profile of equivalent plastic strains after the SMAT process for ball diameters of 1 mm at various speeds.

It can be observed that as the speed increases from 4 m/s to 10 m/s for a 1 mm diameter shot, the equivalent plastic strain on the surface increases from 0.05 to 0.06. The depth of target material, affected by plastic deformation, increases as the ball speed increases. It can be concluded that, generally, an increase in shot speed will significantly influence the depth of effective plastic strain.

The phenomenon of work hardening is another benefit of SMAT, which is due to the localized plastic deformation in the target material caused by the impact of the shots. These impacts and plastic strains reduce grain size and increase the dislocation density on the surface. Consequently, these locked dislocations cause the work hardening of the part. Therefore, with the increasing speed of shot particles and reduced microstructure, it can be concluded that the yield strength and material hardness can increase according to the Hall-Petch theory. The Equations of the Hall-Petch theory are as below:

$$\sigma_y = \sigma_0 + kd^{-\frac{1}{2}} \tag{2}$$

$$H = H_0 + kd^{-\frac{1}{2}} \tag{3}$$

In these Equations, σ_y represents the yield stress, σ_0 is the material's constant for the starting stress for dislocation movement, d is the grain diameter, and k is a constant related to the influence of grain boundaries on dislocation movement. In this Equation, H denotes the material hardness, H_0 is the hardness constant of the Equation, d is the grain diameter, and k is another constant. As the grains become smaller, the material's strength and hardness increase because the number of grain boundaries rises. These boundaries act as obstacles to dislocation movement, thereby enhancing the material's strength. Further increases in dislocation density behind the grain boundaries lead to greater work hardening, contributing to additional strengthening mechanisms and increased material strength.

4.3. Effect of Speed on Displacement in The Depth of The Target Material

Figure 7 shows the amount of displacement caused by indentations for a particle with a diameter of 2 mm at speeds of 4, 8, and 10 m/s. According to the Figure, it is clear that the amount of displacement at the surface of the material is the highest. The amount of displacement has increased with increasing impact velocity, such that the maximum amount of displacement is related to the velocity of 10 meters per second with a magnitude of 0.06 mm. At all three speeds, the amount of displacement has decreased with a similar pattern as it moves into depth. Creating displacement at the surface increases the density of the dislocations and increases the strength of the surface in the SMAT process.

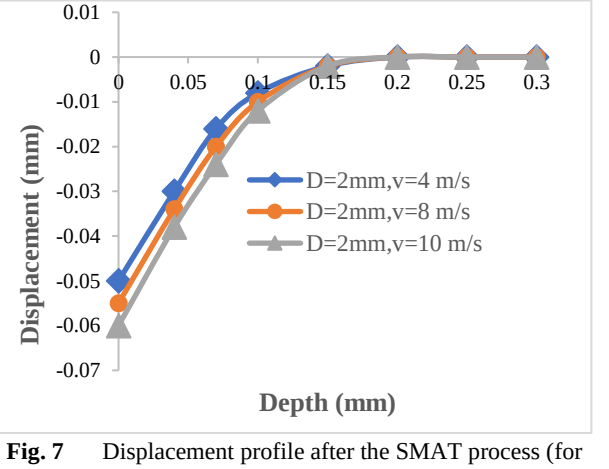

Fig. 7 Displacement profile after the SMAT process (for ball diameter 2 mm at speeds of 4, 8, and 10 m/s).

4 CONCLUSIONS

The effects of steel ball impacts on changes in compressive residual stresses and effective plastic strain in AZ31 magnesium alloy were analyzed using dynamic finite element methods with explicit integration, and evaluated using ABAQUS. The results obtained from this study are as follows:

1. Effect of ball diameter and speed: Increasing the ball diameter and speed has a positive impact on increasing the residual stress and plastic strain values of the material. However, the effect of increasing ball speed on maximum compressive residual stress is greater than the effect of increasing the ball diameter. This is due to the squared effect of speed on translational kinetic energy ($E = 1/2mv^2$), as the impact of speed on kinetic energy is more significant than mass.
2. Compressive residual stress trends: The maximum compressive residual stress increases from

155MPa to 176MPa when the ball diameter is increased from 1 to 3mm at a speed of 4 m/s. Increasing the speed from 4 to 10m/s, for 1 mm ball diameter, raises the maximum compressive residual stress from 155 MPa to 202 MPa. It can be concluded that increasing the diameter from 1 to 3mm has increased the amount of residual stress by up to 13%, while increasing the speed from 4 to 10m/s has increased the amount of residual stress by up to 30%.

3. Impact of SMAT process: The surface residual stress, maximum compressive residual stress, and depth of residual stress penetration, which indicate the effectiveness of the SMAT process, increase with the ball diameter and speed.

4. Improvement of Alloy Properties: The impacts and plastic strains reduce grain size and increase the dislocation density on the surface. Increasing the speed of shot particles and reducing microstructure size increase the material strength and surface hardness. The highest increase in strength can be achieved with a 3 mm diameter ball at a speed of 10 m/s.

5. Optimal conditions: The highest surface residual stress and maximum compressive residual stress are achieved with a 3 mm diameter ball at a speed of 10 m/s. The effect of ball speed on maximum compressive residual stress and depth of penetration is greater than the effect of ball diameter. This is because maximum compressive residual stress is controlled by the material's yield strength, while deformation depth is controlled by plastic strain and strain. As the dynamic stresses from the ball impact the target material, changes in maximum compressive residual stress below the surface decrease.

REFERENCES

[1] Lu, K., J. Lu, Nanostructured Surface Layer on Metallic Materials Induced by Surface Mechanical Attrition Treatment, Materials Science and Engineering: A, Vol. 375, 2004, pp. 38–45.

[2] Liu, G., Lu, J., and Lu, K., Surface Nanocrystallization of 316l Stainless Steel Induced By Ultrasonic Shot Peening, Materials Science and Engineering: A, Vol. 286, No. 1, 2000, pp. 91–95.

[3] Al-Obaid, Y., The Use of Shot Peening Technology In an Aircraft Industry, Third Conf. on Aeronautical Sciences and Aviation Technology, 1989, pp. 4–6.

[4] Shaw, M. C., DeSalvo, G. J., On the Plastic Flow Beneath A Blunt Axisymmetric Indenter, Vol. 92. 1970, pp. 450.

[5] Zhang, X., Lu, J., and Shi, S., A Computational Study of Plastic Deformation in AISI 304 Induced By Surface Mechanical Attrition Treatment, Mechanics of Advanced Materials and Structures, Vol. 18, No. 8, 2011, pp. 572–577.

[6] Meguid, S., Shagal, G., and Stranart, J., 3D FE Analysis of Peening of Strain-Rate Sensitive Materials Using Multiple Impingement Model, International Journal of Impact Engineering, Vol. 27, No. 2, 2002, pp. 119–134.

[7] Todaka, Y., Umemoto, M., and Tsuchiya, K., Comparison of Nanocrystalline Surface Layer in Steels Formed by Air Blast and Ultrasonic Shot Peening, Materials Transactions, Vol. 45, No. 2, 2004, pp. 376–379.

[8] Chaise, T., and et al., Modelling of Multiple Impacts for The Prediction of Distortions and Residual Stresses Induced by Ultrasonic Shot Peening (USP), Journal of Materials Processing Technology, Vol. 212, No. 10, 2012, pp. 2080–2090.

[9] Astaraee, A. H., et al., Incorporating the Principles of Shot Peening for A Better Understanding of Surface Mechanical Attrition Treatment (SMAT) by Simulations and Experiments, Materials & Design, Vol. 116, 2017, pp. 365–373.

[10] Yin, F., and et al., Numerical Modelling and Experimental Approach for Surface Morphology Evaluation During Ultrasonic Shot Peening, Computational Materials Science, Vol. 92, 2014, pp. 28–35.

[11] Manchoul, S., and et al., A Predictive Approach to Investigate the Effect of Ultrasonic Shot Peening on A High-Cycle Fatigue Performance of an AISI 316L target, The International Journal of Advanced Manufacturing Technology, Vol. 95, No. 9, 2018, pp. 3437–3451.

[12] Meng, X., and et al., The Deformation Behavior of AZ31 Mg Alloy With Surface Mechanical Attrition Treatment, Materials Science and Engineering: A, Vol. 707, 2017, pp. 636–646.

[13] Zhang, H., and et al., Formation of Nanostructured Surface Layer on AISI 304 Stainless Steel by Means of Surface Mechanical Attrition Treatment, Acta Materialia, Vol. 51, No. 7, 2003, pp. 1871–1881.

[14] Bagherifard, S., and et al., Experimental and Numerical Analysis of Fatigue Properties Improvement in A Titanium Alloy by Shot Peening, Engineering Systems Design and Analysis, Vol. 49163, 2010, pp. 317–322.

[15] Anand Kumar, S., Ganesh Sundara Raman, S., and Sankara Narayanan, T., Effect of Surface Mechanical Attrition Treatment on Fatigue Lives of Alloy 718, Transactions of the Indian Institute of Metals, Vol. 65, No. 5, 2012, pp. 473–477.

[16] Majzoobi, G., Azizi, R., and Nia, A. A., A Three-Dimensional Simulation of Shot Peening Process Using Multiple Shot Impacts, Journal of Materials Processing Technology, Vol. 164, 2005, pp. 1226–1234.

[17] Liu, Y., Lv, S. L., and Zhang. W., Shot Peening Numerical Simulation of Aircraft Aluminum Alloy Structure, IOP Conference Series: Materials Science and Engineering, Vol. 322, 2018, pp. 032003.

[18] Yarar, E., Erturk, A. T., and Karabay, S., Dynamic Finite Element Analysis on Single Impact Plastic Deformation Behavior Induced by SMAT Process in 7075-T6 Aluminum Alloy, Metals and Materials International, Vol. 27, No. 8, 2021, pp. 2600–2613.

[19] Cao, L.J., Li, S. J., and Shangguan, Z. C., Numerical Simulation of Residual Stresses Induced from Shot Peening with Finite Element Method, Applied Mechanics and Materials, Vol. 433, 2013, pp. 1898–1901.

[20] Hong, T., Ooi, J., and Shaw, B., A Numerical Simulation to Relate the Shot Peening Parameters to the Induced Residual Stresses, Engineering Failure Analysis, Vol. 15, No. 8, 2008, pp. 1097–1110.

[21] Xiao, X., and et al., Prediction of Shot Peen Forming Effects with Single and Repeated Impacts, International Journal of Mechanical Sciences, Vol. 137, 2018, pp. 182–194.

[22] Lei, W., and et al., Effect of Nanocrystalline Surface and Iron-Containing Layer Obtained by SMAT on Tribological Properties of 2024 Al Alloy, Rare Metal Materials and Engineering, Vol. 44, No. 6, 2015, pp. 1320–1325.

[23] Chen, G., and et al., Effects of Strain Rate on The Low Cycle Fatigue Behavior of AZ31B Magnesium Alloy Processed by SMAT, Journal of Alloys and Compounds, Vol. 735, 2018, pp. 536–546.

[24] Peng, J., and et al., The Effect of Surface Mechanical Attrition Treatment on Texture Evolution and Mechanical Properties of AZ31 Magnesium Alloy, Materials Characterization, Vol. 148, 2019, pp. 26–34.

[25] Tomczak, J., Pater, Z, and Bulzak, T., Thermo-Mechanical Analysis of A Lever Preform Forming from Magnesium Alloy AZ31, Archives of Metallurgy and Materials, Vol. 57, No. 4, 2012, pp. 1211–1218.

[26] Hou, X., and et al., A Systematic Study of Mechanical Properties, Corrosion Behavior And Biocompatibility of AZ31B Mg Alloy After Ultrasonic Nanocrystal Surface Modification, Materials Science and Engineering: C, Vol. 78, 2017, pp. 1061–1071.

[27] Mukai, T., and et al., Ductility Enhancement in AZ31 Magnesium Alloy by Controlling Its Grain Structure, Scripta Materialia, Vol. 45, No. 1, 2001, pp. 89–94.

[28] Meguid, S., and et al., Three-Dimensional Dynamic Finite Element Analysis of Shot-Peening Induced Residual Stresses,Finite Elements in Analysis and Design, Vol. 31, No. 3, 1999, pp. 179–191.

[29] Kumar, S., Chattopadhyay, K., and Singh, V., Effect of Ultrasonic Shot Peening on LCF Behavior of the Ti–6Al–4V Alloy, Journal of Alloys and Compounds, Vol. 724, 2017, pp. 187–197.

[30] Bagherifard, S., Ghelichi, R., and Guagliano, M., Mesh Sensitivity Assessment of Shot Peening Finite Element Simulation Aimed at Surface Grain Refinement, Surface and Coatings Technology, Vol. 243, 2014, pp. 58–64.